Calculated and measured reflectivity of $ZnGeP_2$

Carmen Varea de Alvarez,*† Marvin L. Cohen,* S. E. Kohn, Y. Petroff, and Y. R. Shen
Department of Physics, University of California, Berkeley, California 94720
and Inorganic Materials Research Division, Lawrence Berkeley Laboratory, Berkeley, California 94720
(Received 24 June 1974)

Reflectivity spectra of the chalcopyrite ternary compound $ZnGeP_2$ are studied experimentally and theoretically. The measurements of the reflectivity in both the complete parallel and perpendicular polarizations are made at 5 °K. A full zone energy-band structure, the reflectivity and imaginary part of the frequency-dependent dielectric function are calculated using the empirical pseudopotential method. Comparison is made with the measured reflectivity and modulated reflectivity and prominent features in the experimental spectra are identified and associated with interband transitions. In addition, spin-orbit interactions are included at a few points of the Brillouin zone.

I. INTRODUCTION

Recently, much attention has been given to studies of the electronic and optical properties of ternary chalcopyrite compounds with chemical formula $A^{N-1}B^{N+1}C_2^{8-N}$ ($N=3, 2$). We report here the results of experimental and theoretical investigations into the properties of $ZnGeP_2$. This material is treated as a model for the chalcopyrite semiconductors. The measurements include detailed reflectivity and modulated reflectivity data for incident light both in the completely parallel and perpendicular polarizations (with respect to the tetragonal axis). Details of the experimental procedures are given in Sec. II (modulated reflectivity and ordinary reflectivity data are in Figs. 1 and 2, respectively). Theoretical details are in Sec. III. The rest of the paper describes and discusses the results.

Theoretically, the study of the electronic and optical properties of these compounds is a logical extension of the study of their closest analogs the $B^N C^{8-N}$ ($N=3, 2$) zinc-blende semiconductors. The $A^{N-1}B^{N+1}C_2^{8-N}$ have many interesting physical properties which promise to be useful for studies of the electronic properties of semiconductors in general and for applications to semiconductor technology.

The chalcopyrites also have good nonlinear optical properties and have been considered for application in the infrared.[1] In the case $N=3$ most of these ternary compounds crystalize in the chalcopyrite structure which is a simple generalization of the zinc-blende, crystal structure. We know from the experimental properties and from the theoretical work of Cohen and Bergstresser,[2] and Phillips and Van Vechten[3] that most of the electronic and optical properties of the B^3C^5 zinc-blende semiconductors are analogous to those of the diamond-structure semiconductors (group B^4). Some modifications exist when the effects of the anion and cation difference are introduced into the band structure and bonding properties. In the same way, most of the properties of $A^2B^4C_2^5$ chalcopyrite semiconductors can be understood by introducing the effects of the differences of the two cations A and B and the small distortion parameter (σ) of the anion C into the band structure of their zinc-blende analog. This is done by breaking up the crystalline pseudopotential into a zinc-blende part and two chalcopyrite modification terms due to the difference between A and B, and the displacement of C. The electronic band structure for $ZnGeP_2$ is then calculated using the empirical pseudopotential method. In addition, we have calculated the imaginary part of the frequency dependent dielectric function $\epsilon_2(\omega)$ and the reflectivity spectrum $R(\omega)$.

As discussed in Sec. III, pseudopotential form factors for $ZnGeP_2$ were extracted from GaP form factors[4] and Ge form factors[2] and no experimental information (except lattice parameters) was used to obtain the electronic band structure of this chalcopyrite compound. Spin-orbit interactions were included at a few points of the Brillouin zone using the method of Weisz[5] as modified by Bloom and Bergstresser.[6]

Comparison of the calculated and measured re-

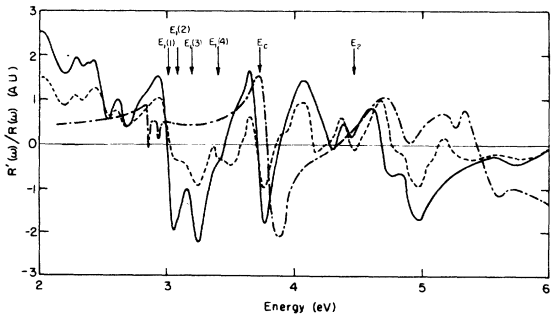

FIG. 1. Derivative spectra $(1/R)dR/d\omega$ of $ZnGaP_2$ at 5 °K for parallel (solid line) and perpendicular (dashed line) polarization. For comparison the derivative spectra of GaP (dot-dashed line) is given.

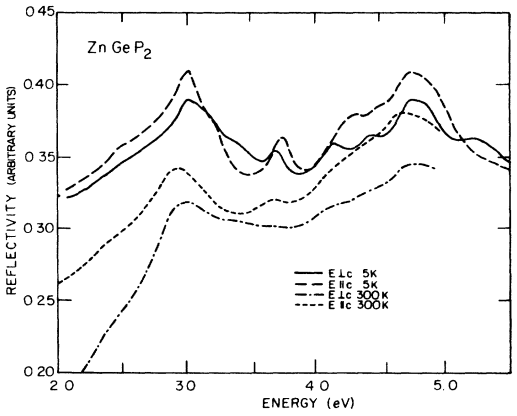

FIG. 2. Reflectivity of $ZnGeP_2$ at 5 and 300 °K.

flectivity spectra shows that our model gives most of the prominent optical structure but the calculated structure is shifted by about 0.3 eV to higher energies. Better agreement can be expected if the form factors are slightly adjusted. This comparison also allows us to identify the interband transitions responsible for the prominent structure in the reflectivity, thus making it possible to extract all the pertinent information that the experimental reflectivity gives on the direct interband transitions.

II. EXPERIMENT

The reflectivity $R(\omega)$ and the logarithmic derivative of the reflectivity $(1/R)\, dR/d\omega$ have been mea-

TABLE I. Theoretical and experimental reflectivity structure and their identifications, including the location in the Brillouin zone and energy of the calculated critical points for $ZnGeP_2$.

Theoretical Peak position (eV)	Reflectivity structure: Experimental Peak position (eV) (a)	(b)	(c)	(d)	Polarization (a)	Peak	Location in zone	cp energy (eV)
		2.08[e]				A'	Γ_4-Γ_3	
		2.145[e]		2.05		B'		
	2.14				∥, ⊥		Γ_5-Γ_3	
		2.21[e]		2.11	⊥	C'		
	2.29					B''		
		2.3[e]					Γ_5-Γ_2	
	2.31				∥	C''		
2.31	2.51	2.46	2.39	2.34	∥, ⊥	A	Γ_2^--Γ_1^-	2.31[f]
2.27	2.63	2.53	2.46	2.40	⊥	B	Γ_1^--Γ_1^-	2.27[f]
2.43	2.67	2.59	2.52	2.48	∥	C	Γ_2^--Γ_1^-	2.43[f]
3.04					∥		X_1-X_1(15, 16-17, 18)	3.04 {3.50[f] 3.03[f]}
3.41	3.02	3.02	2.97	2.87 (2.92)	∥, ⊥	$E_1(1)$	N_1-N_1(16-17) (0.2, 0.2, 0.4)	3.42[f]
3.37					⊥		X_1-X_1(13, 14-17, 18)	3.36 {3.35[f] 3.37[f]}
3.41	3.08	3.15	3.09	3.05	⊥, ∥	$E_1(2)$	N_2-N_1(15-17) (0.2, 0.2, 0.4)	3.50[f]
3.6	3.2	3.22	3.13	3.32	⊥(∥)	$E_1(3)$	N_2-N_1(16, 17) (0.3, 0.3, 0.38)	3.6
3.9	3.41	3.48	3.41	3.64	⊥	$E_1(4)$	Σ_2-Σ_1(16, 18) (0.25, 0.25, 0)	3.95
4.0	3.74 (3.72)	3.75	3.71	3.83	∥(⊥)	E_c	X_1-X_1(11, 12, 17, 18)	3.9
4.6	4.17				⊥		Λ(13-17)(0, 0, 0.6) Σ(14-17) (0.25, 0.25, 0)	4.6
4.76	4.3				∥		Δ(15-17)(0.34, 0, 0)	4.76
4.77	4.46				⊥	E_2	Γ-Γ(13-18)	4.77
5.05	4.73				∥		(14-17)(0.16, 0.5, 0)	5.05
4.96	4.79				⊥		X(16-20) and along Σ	4.96
5.21	4.92	(4.93)			∥(⊥)		Δ(15-18)(0.5, 0, 0)	5.21

[a]This work at 5 °K.
[b]Thermoreflectance work of Shileika at 120 °K (Ref. 16).
[c]Electroreflectance work of Shileika at 300 °K (Ref. 14).
[d]Electroreflectance work of Shay at 300 °K (Ref. 14).
[e]Wavelength-modulated absorption work of Shileika at 77 °K (Ref. 16).
[f]Spin-orbit Hamiltonian included.

sured using our wavelength-modulation spectrometer.[7] The modulating frequency is 1 kHz. Double-beam optics with proper feedback loops were used to eliminate the large unwanted background in the derivative spectrum. Details of the electronic and optical instrumentation have been given elsewhere.[7]

The sample of $ZnGeP_2$ was a large single crystal obtained from Rockwell International Corp. The crystal was cut parallel to the {100} face. It was then mechanically polished and etched with "Syton." This produced a flat surface with a bluish-metallic appearance. The crystal was then mounted on a copper sample holder and was kept in a helium atmosphere in an optical Dewar. This allowed us to work for long periods of time at low temperatures without contamination or deterioration of the surface.

The experimental $(1/R)\ dR/d\omega$ spectra at 5 °K are presented in Fig. 1 for light polarized parallel and perpendicular to the c axis of the crystal. For comparison, the modulation spectrum of GaP,[8] the III-V analog of $ZnGeP_2$, is also presented. The reflectivity at 5 and at 300 °K for both polarizations is shown in Fig. 2. As can be seen, the reflectivity spectra are dominated by two main peaks around 3.0 and 4.7 eV and a weaker structure at about 3.7 eV. Following the notation of Stokowski[9] for several other II-IV-VI_2 compounds, the two main structures are labeled E_1 and E_2 and the third peak is labeled E_c. The E_1 and E_2 peaks are composed of several subsidiary structures. Table I lists the observed structures along with their experimental and theoretical energies and their assignment to transitions in the Brillouin zone.

III. CALCULATIONS AND RESULTS

The pseudopotential Hamiltonian for an electron in the crystal is

$$H = -(\hbar^2/2m)\nabla^2 + V(\vec{r}) , \tag{1}$$

where $V(\vec{r})$ is the weak crystalline pseudopotential that can be expanded in reciprocal-lattice vectors $\vec{G}$,

$$V(\vec{r}) = \sum_{\vec{G}} e^{-i\vec{G}\cdot\vec{r}} V(\vec{G}) ,$$

where

$$V(\vec{G}) = \frac{1}{8}\sum_a e^{i\vec{G}\cdot\vec{\tau}_a} V_a(\vec{G}) . \tag{2}$$

τ_a is the vector which locates each atom in a primitive cell and $V_a(\vec{G})$ is the Fourier transform of the atomic pseudopotential for atoms of kind a, which is assumed spherically symmetric:

$$V_a(\vec{G}) = \frac{1}{\Omega}\int V_a(\vec{r})\, e^{i\vec{G}\cdot\vec{r}}\, d^3r . \tag{3}$$

Ω is the atomic volume. $ZnGeP_2$ crystallizes in a body-centered-tetragonal structure with eight atoms in the primitive cell; the basis is given by

$$\text{Zn:}\quad \vec{\tau}_1^{Zn} = (0, 0, 0), \qquad \vec{\tau}_2^{Zn} = (0, \tfrac{1}{2}a, \tfrac{1}{4}c) ,$$

$$\text{Ge:}\quad \vec{\tau}_1^{Ge} = (0, 0, \tfrac{1}{2}c), \qquad \vec{\tau}_2^{Ge} = (0, \tfrac{1}{2}a, \tfrac{3}{4}c) ,$$

$$\text{P:}\quad \vec{\tau}_1^{P} = (au, \tfrac{1}{4}a, \tfrac{1}{8}c), \qquad \vec{\tau}_2^{P} = (a\bar{u}, \tfrac{3}{4}a, \tfrac{1}{8}c),$$

$$\vec{\tau}_3^{P} = (\tfrac{3}{4}a, au, \tfrac{7}{8}c), \qquad \vec{\tau}_3^{P} = (\tfrac{1}{4}a, a\bar{u}, \tfrac{7}{8}c),$$

where $a = 5.46$ Å, $c = 10.71$ Å, $u = 0.2582$ at room temperature.[10]

The space group is the nonsymmorphic group D_{2d}^{12} (body-centered-tetragonal lattice) and the unit cell (see Fig. 3) can be thought of as composed of two zinc-blende unit cells (volume a^3) stacked and compressed along the z axis. A primitive cell of the chalcopyrite structure (volume $\frac{1}{2}ac^2$) contains four primitive cells of the zinc blende (volume $\frac{1}{4}a^3$). The cation of the zinc blende is substituted by the two cations of the chalcopyrite in such a way that two kinds of chains are formed. Zn-P-Ge-P-Zn chains run along the $(1, \pm 1, 0)$ directions while Zn-P-Zn-P-Ge-P-Ge-P-Zn chains run along the $(0, \pm 1, 1)$ and $(\pm 1, 0, 1)$ directions. The presence of Zn-P-Zn and Ge-P-Ge linkages along the z axis is responsible for the doubling of the unit cell with respect to the zinc-blende case. The lattice is slightly compressed along the z axis, this tetragonal compression being measured by the parameter $\epsilon = 2 - c/a$. The anion of $ZnGeP_2$ is tetrahedrally coordinated to two Zn and two Ge atoms and slightly displaced from the centers towards the smaller pair of cations (the Ge atoms); this displacement can be measured by the small parameter $\sigma = 4u - 1$. The zinc-blende and the chalcopyrite structures are similar. The first Brillouin zone (BZ) of the chalcopyrite can be obtained by folding down the first BZ of the zinc blende (see Fig. 4). The $\vec{G}$ vectors used in the folding-in process are $\vec{\Gamma} = (0, 0, 0)$, $\vec{W}_x = (1, 0, 1)$, $\vec{W}_y = (0, 1, 1)$ and $\vec{X}_z = (0, 0, 2)$.[11]

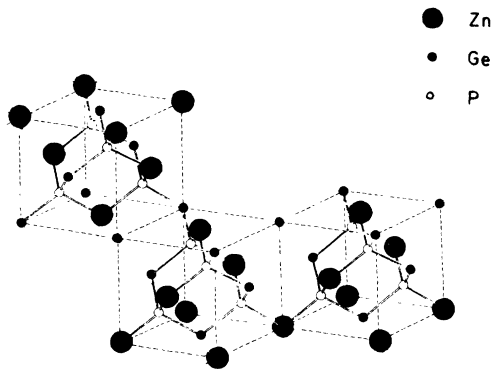

FIG. 3. Crystal structure of $ZnGeP_2$.

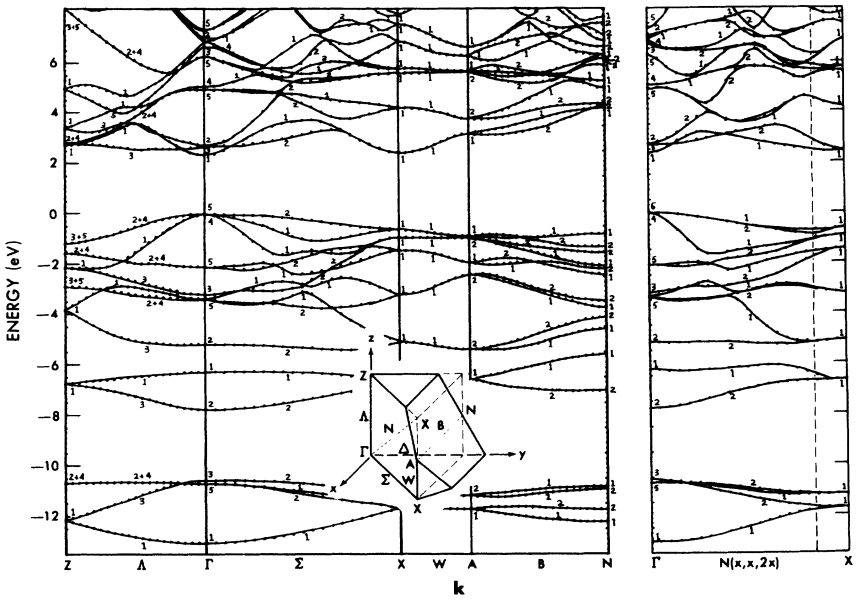

FIG. 4. Band structure for $ZnGeP_2$ along the principal symmetry directions. In the text the bands are numbered consecutively 1–16 for valence bands and 17 onward for the conduction bands.

It is easy to show that the set of $\vec{G}$ vectors of the chalcopyrite structure can be broken into four different sets related to the zinc-blende $\vec{G}$' s of the form $\vec{G}=\vec{G}_{zb}+\vec{\Gamma}$, $\vec{G}=\vec{G}_{zb}+\vec{W}_x$, $\vec{G}=\vec{G}_{zb}+\vec{W}_y$, and $\vec{G}=\vec{G}_{zb}+\vec{X}_z$.

Some of the ternary crystals with composition $A^2B^4C^5$ (e.g., $MgGeP_2$), lack the segregation of their two cations. The cations are considered randomly distributed among the cation position in the zinc-blende analog. Then the compound has the zinc-blende structure; one of the two sites in the primitive cell is occupied by the anion and the other by an average of the two cations ($A^2+\frac{1}{2}B^4$). It is mainly the ordering of the two cations and their different potentials which distinguishes the chalcopyrite from the zinc-blende (zb) structure. In view of this, it is instructive to decompose the crystalline pseudoptoential in reciprocal space [Eq. (2)] into a zb component which includes the average of the two cation potentials and another which takes into account the modification due to the chalcopyrite structure

$$\begin{aligned} V_1(\vec{G}) &= \tfrac{1}{2}[V_{Zn}(\vec{G})+V_{Ge}(\vec{G})]\,, \\ V_2(\vec{G}) &= V_P(\vec{G})\,, \\ V_A^c(\vec{G}) &= \tfrac{1}{2}[V_{Zn}(\vec{G})-V_{Ge}(\vec{G})]\,, \end{aligned} \tag{4}$$

where V_1 is the average and $2V_A^c$ is the difference of the two cation potentials. We also define the vectors β_i ($i=1,4$) to specify the displacement of the anions

$$\begin{aligned} \vec{\beta}_1 &= \vec{\tau}_1^{\,P}-\vec{\sigma}_1\,, \quad \vec{\beta}_2=\vec{\tau}_2^{\,P}+\vec{\sigma}_2\,, \\ \vec{\beta}_3 &= \vec{\tau}_3^{\,P}-\vec{\sigma}_3\,, \quad \vec{\beta}_4=\vec{\tau}_4^{\,P}+\vec{\sigma}_4\,, \end{aligned}$$

where $\vec{\sigma}_1=(\sigma,0,0)a/4$, $\vec{\sigma}_2=-\vec{\sigma}_1$, $\vec{\sigma}_3=\frac{1}{4}(0,\sigma,0)a$, and $\vec{\sigma}_4=-\vec{\sigma}_3$ represent the displacement of the P atoms from their original sites in the zb analog. With this, Eq. (2) can be written in the form

$$\begin{aligned} V(\vec{G}) &= \tfrac{1}{8}V_{Zn}(\vec{G})\sum_{i=1}^{2}e^{i\vec{\tau}_i^{Zn}\cdot\vec{G}}+\tfrac{1}{8}V_{Ge}(\vec{G})\sum_{i=1}^{2}e^{i\vec{\tau}_i^{Ge}\cdot\vec{G}}+\tfrac{1}{8}V_2(\vec{G})\sum_{i=1}^{4}e^{i\vec{\tau}_i^{P}\cdot\vec{G}} \\ &= \tfrac{1}{8}V_1(\vec{G})\left(\sum_{i=1}^{2}e^{i\vec{\tau}_i^{Zn}\cdot\vec{G}}+\sum_{i=1}^{2}e^{i\vec{\tau}_i^{Ge}\cdot\vec{G}}\right)+\tfrac{1}{8}V_2(\vec{G})\sum_{i=1}^{4}e^{i\vec{\beta}_i\cdot\vec{G}} \\ &\quad +\tfrac{1}{8}V_A^c(\vec{G})\left(\sum_{i=1}^{2}e^{i\vec{\tau}_i^{Zn}\cdot\vec{G}}-\sum_{i=1}^{2}e^{i\vec{\tau}_i^{Ge}\cdot\vec{G}}\right)+\tfrac{1}{8}V_2(\vec{G})\sum_{i=1}^{4}e^{i\vec{\beta}_i\cdot\vec{G}}(e^{i\vec{\sigma}_i\cdot\vec{G}}-1)\,. \end{aligned} \tag{5}$$

As is customary in the zb case, let us define

$$V_S(\vec{G})=\tfrac{1}{2}[V_1(\vec{G})+V_2(\vec{G})]=\tfrac{1}{4}[V_{Zn}(\vec{G})+V_{Ge}(\vec{G})+2V_p(\vec{G})]$$

and

$$V_A(\vec{G})=\tfrac{1}{2}[V_1(\vec{G})-V_2(\vec{G})]=\tfrac{1}{4}[V_{Zn}(\vec{G})+V_{Ge}(\vec{G})-2V_p(\vec{G})]\,. \tag{6}$$

We then have, from the first two terms on the right-hand side of Eq. (5) the zb part of the potential:

$$V_{zb}(\vec{G}) = e^{i\vec{G}\cdot\vec{\eta}}[S_S(\vec{G})V_S(\vec{G}) + iS_A(\vec{G})V_A(\vec{G})] .$$

Here, the structure factors $S_S(\vec{G})$ and $S_A(\vec{G})$ are the usual symmetric and antisymmetric structure factors of the zb structure (compressed along the c axis); the phase factor $e^{i\vec{G}\cdot\vec{\eta}}$ only shifts the origin to the Zn atoms (the usual origin in the zb case is halfway between the two atoms in the cell).

Since it is expected that the electronic properties of $ZnGeP_2$ should closely resemble those of its zb analog GaP in the present calculation we used $V_s(\vec{G}) = V_s^{GaP}(\vec{G})$ and $V_A(\vec{G}) = V_A^{GaP}(\vec{G})$. The GaP form factors used were obtained from Ref. 4, the Ge form factors used from Ref. 2, and the Zn and P form factors extracted from Eqs. (6). The pseudopotential curves of $V_i(|\vec{G}|)$ vs $|\vec{G}|$ were free hand extrapolated and renormalized to the atomic volume of $ZnGeP_2$ [see Eq. (3)].

The third term on the right-hand side of Eq. (5) which is due to the difference between the potentials of the two cations, can be written in the form

$$V_a^c(\vec{G}) = S_A^c(\vec{G})V_A^c(\vec{G}) . \tag{7}$$

The structure factor $S_A^c(\vec{G})$ can be reduced to the form [see Eq. (5)]

$$S_A^c(\vec{G}) = -\tfrac{1}{2} i e^{i\vec{\tau}_2^{Ge}\cdot\vec{G}/2} \times \sin(\vec{\tau}_1^{Ge}\cdot\tfrac{1}{2}\vec{G})\cos(\vec{\tau}_2^{Zn}\cdot\tfrac{1}{2}\vec{G}) . \tag{8}$$

The last term on the right hand side of Eq. (5) is due to the displacement of the anion and depends only on the pseudopotential form factors of the anion and on the distortion parameter σ. We put the term in the form

$$V_u(\vec{G}) = V_p(\vec{G})S_u(\vec{G}) , \tag{9}$$

where the structure factor $S_u(\vec{G})$ is

$$S_u(\vec{G}) = \frac{1}{8}\sum_{i=1}^{4} e^{i\vec{\beta}_i\cdot\vec{G}}(e^{i\vec{\sigma}_i\cdot\vec{G}} - 1) . \tag{10}$$

Since $\sigma \sim 0.1$ for most of the $A^2B^4C_2^5$ chalcopyrite compounds in which the u parameter has been measured, Eq. (10) shows that the structure factors $S_u(\vec{G})$ are small in the region in reciprocal space where the pseudopotentials are appreciably different from zero [$|q| \leq 4(2\pi/a)$]. From the above it should be clear that the effects of $V_u(\vec{G})$ on the band structure are expected to be small. On the other hand, the nonzero $S_A^c(\vec{G})$ are of the order of one-fourth of the nonzero $S_S(\vec{G})$ or $S_A(\vec{G})$.

One can understand the band structure of the chalcopyrite compounds as a modification of the band structure of their zinc-blende analogs. To do that one proceeds as follows: (i) The band structure of the zinc-blende analog is first folded into the smaller chalcopyrite Brillouin zone. (ii) In the fold-in process, each $\vec{k}_{chal}$ vector in the first chalcopyrite BZ corresponds to four different $\vec{k}_{zb}$ vectors in the first zinc-blende BZ. (iii) In "turning on" the "chalcopyrite perturbation," the states at $\vec{k}$, $\vec{k}+\vec{W}_x$, $\vec{k}+\vec{W}_y$, and $\vec{k}+\vec{X}_z$ in the zinc-blende BZ are mixed. Since $S_A^c(\vec{G})$ is nonzero only for $\vec{G} = \vec{G}_{zb} + \vec{W}_x$ or $\vec{G} = \vec{G}_{zb} + \vec{W}_y$, the pseudopotential $V_a^c(\vec{G})$ mixes only those k states that differ by $\vec{W}_x$ or $\vec{W}_y$. One expects big changes in the band structure at points such as the crossing point of the W-L and Γ-Σ lines in the conduction band along the Σ direction of the chalcopyrite BZ or at $X[\Sigma(\frac{1}{2}, \frac{1}{2}, 0), L]$ at the top of the valence band where the energies of the Σ_2 and L_3 levels are very close to each other. (iv) The structure factors $S_u(\vec{G})$ are nonzero for all the four subsets of $\vec{G}$, but we have shown that the pseudopotential $V_u(\vec{G})$ is expected to be small, and so, the mixing of $\vec{k}$ and $\vec{k}+X_z$ states should be small. One of the consequences is that the $\Gamma_4 + \Gamma_5(\Gamma_{15}) - \Gamma_3(X_1)$[12,13] pseudo-direct transitions[14,15] are very weak. These transitions are only observable by optical modulation techniques when they constitute the first absorption edge of the crystal.[14,16]

In solving for the eigenvalues and eigenvectors of the *full* Hamiltonian, we expanded the wave functions into a set of 69-84 plane waves; 244 additional plane waves were used through the perturbation scheme developed by Lowdin.[17] The energies and wave functions were calculated in $\frac{1}{16}$ of the BZ at 288 grid points, and the $\epsilon_2(\omega)$ integration over k space was performed by the method developed by Gilat and Raubenheimer[18] in what we call the practical Brillouin zone (PBZ). The PBZ was chosen because it can easily be shown that the region in k space surrounded by the planes $k_z = 0$, $k_z = 2\pi/c$, $k_z = k_y$, $k_y = 0$, and $k_z = \pi/a$ is completely equivalent to the usual irreducible part of the BZ (i.e., $\frac{1}{16}$ of the full BZ).

Spin-orbit corrections were carried out at a few points in the BZ by extending the zinc-blende calculation.[5,6] The fact that we are dealing with three kinds of atoms and eight atoms in the primitive cell presents no problem. We use the two ratios of the cations to the anion spin-orbit contributions given in Ref. 19; this leaves us with one spin-orbit parameter which we choose to be that of Ge. The usual procedure is to fit this parameter to the spin-orbit splitting Δ_{so} at the Γ point of the BZ. At the time this calculation was performed, there was no experimental information about Δ_{so} for $ZnGeP_2$, so the parameter we chose was the one that gives the correct spin-orbit splitting for Ge in the diamond structure. The eigenvalues of the spin-orbit Hamiltonian require the diagonalization of a 138×138 matrix and the large amount of computer time involved prohibits spin-orbit calculations over the entire BZ.

A. Optical structure in the E_0 region

The first optical transitions in $ZnGeP_2$ are transitions from the top of the valence band to the bottom of the conduction band at Γ. The Γ_{15} valence band in GaP is split by the crystal-field splitting Δ_{cr} into a doubly degenerate band of Γ_5 symmetry and a singlet band of Γ_4 symmetry. With the addition of spin-orbit interactions, the Γ_5 states split into states of $\Gamma_{\bar{1}}$ and $\Gamma_{\bar{2}}$ symmetry. The first optical transitions with significant oscillator strength are from these three valence-band states to a conduction band of $\Gamma_{\bar{1}}$ symmetry which is the analog of the Γ_1 states in GaP. These transitions, labeled A, B, and C, have been seen and discussed by Shaly[14] and by Shileika.[16] In room-temperature electroreflectance Shay observes these transitions at 2.34, 2.40, and 2.48 eV, respectively. Shileika reports values of 2.46, 2.53, and 2.59 eV also from room-temperature electroreflectance. At 5 °K we observe structures at 2.51, 2.63, and 2.67 eV, and we *tentatively* assign the latter two to B and C. From these values, we calculate values for the spin-orbit splitting of $\Delta_{so} = 0.13$ eV and for the crystal field splitting of $\Delta_{cr} = -0.04$ eV using the quasicubic theory of Hopfield.[20] In our pseudopotential calculation of the $ZnGeP_2$ band structure, we have used the spin-orbit parameter $\Delta_{so} = 0.16$ eV for Ge. We find these transitions at 2.31, 2.27, and 2.43 eV, respectively. The centroid of this triplet, 2.34 eV, is shifted approximately 0.3 eV from the centroid of the experimental energies, which appears to be general for all of the pseudopotential critical point energies we calculate for $ZnGeP_2$. In the more rigorous calculation, we should use the experimental Δ_{so} as a known parameter. The theoretical value of the B peak is less than that of the A peak because we predict a positive crystal field splitting, while the experimental value is negative. First-order perturbation predicts that this quantity depends only on the tetragonal compression of the crystal, and therefore it depends only on the slopes of the pseudopotential curves near the reciprocal-lattice vectors (2, 0, 0), (2, 2, 0), and (3, 1, 2). Since the crystalline tetragonal compression is so small, form factors have to be determined to the third significant figure. Therefore, Δ_{cr} is difficult to predict. It would however be easy to adjust the pseudopotential curves to give the correct crystal-field splitting.

The zinc-blende analog of $ZnGeP_2$ is an indirect gap Γ_{15}-X_1 semiconductor. When the BZ of GaP is folded into the BZ of $ZnGeP_2$, the X_1 states of GaP map into Γ states of $ZnGeP_2$. Furthermore, the effect of $V_A^c(\vec{G}) + V_u(\vec{G})$ is expected to be small near the band edge at Γ because the $\Gamma(W)$ states are far away from the band gap in GaP. Thus it is expected that the lowest interband transition in $ZnGeP_2$ will have a very small oscillator strength, and $ZnGeP_2$ is referred to as a "pseudodirect" gap semiconductor. Moreover, the hydrostatic pressure coefficient is expected to be close to that of the Γ-X edge of GaP (Ref. 21) since this parameter depends only on the symmetry of the wave functions which are almost unaffected by the chalcopyrite potential. All of this has been observed for $ZnGeP_2$. Shileika[16] observes very weak transitions at 2.14 and 2.21 eV, labeled B' and C', in wavelength-modulated absorption at 77 °K. These are assigned to transitions from the spin-orbit split Γ_5 valence band to the Γ_3 conduction band. He also observes the band gap at 2.08 eV with a hydrostatic pressure coefficient of 2.2×10^{-6} eV kg^{-1} cm^2. In electroreflectance, Shileika observes very weak structure at 2.3 eV which is attributed to transitions Γ_5-Γ_2, the analog of the Γ_{15}-X_3 transition in GaP. Shay observes the B' and C' structures at 2.05 and 2.11 eV. In our measurements at 5 K, we observe a small structure at 2.14 eV in both polarizations which agrees well with the results of Shileika. We also observe weak structures at 2.29 eV for perpendicular polarization and 2.31 eV for the parallel polarization. We believe these are the B'' and C'' transitions seen by Shileika.

B. Optical structure in the E_1 region

As shown in Fig. 1, the experimental modulated reflectivity of $ZnGeP_2$ shows much richer structure than that of its analog (GaP). In the E_1 region corresponding to the two spin-orbit split peaks, E_1 and $E_1+\Delta_1$ of GaP, $ZnGeP_2$ has five resolvable structures. In general these splittings are observed in most of the chalcopyrite compounds studied so far.[22] These five structures in the spectrum have been labeled $E_1(1)$, $E_1(2)$, $E_1(3)$, $E_1(4)$, and E_c by Stokowski[9] and E_1, E_2, E_3, E_4, E_6 by Shileika.[16] We will stick to Stokowski's notation. The most important features of these structures are the following: the energy separations $E_1(2)$-$E_1(1)$ and $E_1(3)$-$E_1(4)$ are close to each other for most of the $A^2B^4C_2^5$ crystals studied, this seems to indicate that the first four transitions in the E_1 region come from two spin-orbit split doublets in the same region of the BZ. Both our experimental results and critical point analysis show that this is *not* the case, at least for $ZnGeP_2$. The experimental splitting $E_1(2)$-$E_1(1)$ is 0.06 eV, while the $E_1(4)$-$E_1(3)$ splitting is 0.21 eV. The origin of these structures has been subject to extensive investigation in the last few years. Most interpretations agree in that the $E_1(1)$ and $E_1(2)$ structure originates from transitions in the N plane along the $2\pi(x/a, x/a, 2x/c)$ direction. This is equivalent to the Λ transitions in GaP when one uses a quasicubic

model. Our full-zone calculations for the reflectivity of $ZnGeP_2$, show that this is indeed the case and the critical point is near $x = 0.2$ (Fig. 4). We find that the mixing of the valence bands involved in the transitions under the action of the chalcopyrite part of the pseudopotential is very small, so spin-orbit interaction effects should be very close to those of GaP. Our calculated spin-orbit splitting between the $E_1(1)$ and $E_1(2)$ peaks in $\Delta_1 = 0.08$ eV. In the experimental modulated spectrum its value is $\Delta_1 = 0.06$ eV.

The nature of the $E_1(3)$ and $E_1(4)$ structure is more subject to controversy. Kavaliauskas *et al.*[23] suggest that all four peaks $E_1(1)$ to $E_1(4)$ come from transitions at the X point of the BZ in the bands 15-16 (top valence band) → 17-18 (bottom conduction band) and 13-14 → 17-18. Under the influence of the spin-orbit interactions, each fourfold degenerate level X_1, splits into two twofold degenerate levels $X_1 \rightarrow X_{\bar{1}} + X_{\bar{4}}$, $X_{\bar{2}} + X_{\bar{3}}$. From our studies in $ZnGeP_2$, the splitting $X_{\bar{1}} + X_{\bar{4}} - X_{\bar{2}} + X_{\bar{3}}$ is 0.02 eV. It is thus too small to be associated with the energy separation between $E_1(1)$, $E_1(3)$, and $E_1(2)$, $E_1(4)$ as Kavaliauskas *et al.* suggest. Stokowski[9] assigns the $E_1(3)$ and $E_1(4)$ peaks to transitions at the X point of the BZ, the top of the valence band at the X point of the BZ contains six levels (11–16) which are almost degenerate in a quasicubic model. These six levels correspond to the two fourfold degenerate levels $X_1(L_3)$ [$L_3 = (\frac{1}{2}, -\frac{1}{2}, -\frac{1}{2})2\pi/a$ and $L_3 = (-\frac{1}{2}, \frac{1}{2}, -\frac{1}{2})2\pi/a$] and the fourfold degenerate level $X_1(\Sigma_1)$ [$\Sigma_1 = (\frac{1}{2}, \frac{1}{2}, 0)2\pi/a$, $\Sigma_1 = (-\frac{1}{2}, -\frac{1}{2}, 0)$]. The fact that the L_3 and Σ_1 levels are almost degenerate is not accidental. Cohen and Bergstresser's[2] band structures for the $B^N C^{8-N}$ semiconductors show that the L_3 and Σ_1 levels are always very close in energy. Under these circumstances, the effects of the chalcopyrite part of the pseudopotential mixing the Σ_1 and L_3 levels is expected to be large as shown in Fig. 4. This large interaction and the shifts of L_3^v-to-L_1^c transitions relative to the Λ_3^v to Λ_1^c transitions, underlie the Stokowski[9] suggestion that the $E_1(3)$, $E_1(4)$, and E_c peaks come from transitions at the X point from bands (11, 12), (13, 14), (15, 16) → (17, 18). Even though all of these transitions are allowed due to the strong L-Σ mixing in the valence band, we find that the (15, 16) → (17, 18) transitions at the X point lay below the $\Lambda[E_1(1), E_1(2)]$ peak. The X_1-X_1 transitions [bands (15, 16) → (17, 18)] make some contributions to the $E_1(1)$ peak of our calculated $\epsilon_2(\omega)$ (see Fig. 5), and the X_1-X_1 transitions [bands (13, 14) → (17, 18)] contribute to the $E_1(2)$ peak of our calculated $\epsilon_2(\omega)$.

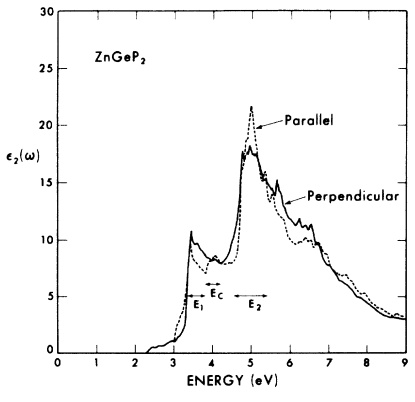

FIG. 5. Theoretical $\epsilon_2(\omega)$ for $ZnGeP_2$ for light polarized parallel and perpendicudlar to the c axis of the crystal.

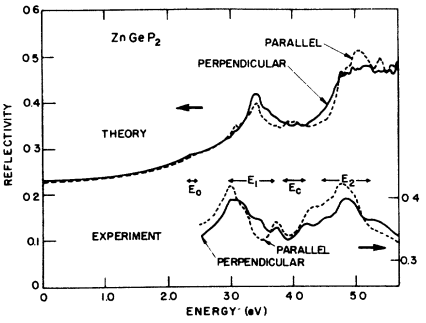

FIG. 6. Comparison of the theoretical and experimental $R(\omega)$ for $ZnGeP_2$ in the parallel and perpendicular polarizations.

In the region corresponding to the $E_1(3)$ and $E_1(4)$ peaks of the experimental reflectivity, we find two pieces of structure mostly in the perpendicular polarization; we find that these two structures come mainly from transitions in the N plane of the BZ. One critical point is close to the point (0.3, 0.3, 0.38) (bands 16-17) and the other is close to (0.25, 0.25, 0) (bands 16-18). These two critical points have the same origin in a quasicubic model. A plot of the folded in band structure of a zinc-blende semiconductor, shows that the (0, 0, 0) to $(\frac{1}{2}, \frac{1}{2}, z)$ line and the (1, 0, 1) to $(\frac{1}{2}, -\frac{1}{2}, z-1)$ line in the first conduction band always cross along a line close to the $(\frac{1}{4}, \frac{1}{4}, 0)$ to $A(\frac{1}{2}, \frac{1}{2}, \frac{1}{2})$ direction; the interaction between these lines is quite strong creating the two critical points mentioned above.

We have been able to associate the E_c structure to transitions at the X point $X_1(\Sigma_2, L_3) \rightarrow X_1(L_1)$, this peak is stronger in the parallel polarization. One has to be cautious when identifying the E_c structure, since it is caused by an M_0 singular point; the actual peak is shifted by about 0.1 eV to higher energies with respect to the energy of the transition at the singularity.

C. Optical structure in the E_2 region

At higher energies, in the region corresponding to the E_2 peak of the reflectivity structure of zinc-blende semiconductors, at least five pieces of structure are observed. In the measured modulated reflectivity of $ZnGeP_2$, we have been able to identify six prominent pieces of structure. Our calculations show that most of the contribution to the E_2 structure comes from transitions in the Δ and Σ directions of the zb analog as expected. The Δ direction folds into the Δ, Λ and $(1-x, 0, 1)$ directions of the chalcopyrite BZ, while the Σ direction is folded into the Σ, $(x, 0, 2x)$, and $(1-x, 0, 2x-1)$ directions. Summation over k space along Δ and Σ directions shows that in effect the E_2 peak is mainly a Δ, Σ peak.

The first peak in the parallel polarization around 4.76 eV comes from transitions along the Δ direction (15–17) at (0.34, 0, 0); the line $\Delta(\Delta)$ mixes with the line $\Delta(1-x, 0, \frac{1}{2})$ in the valence band and then continues into bands (13, 14), so transitions (13, 14)→17 near (0.5, 0.0) also contribute to this peak. In the experimental spectra this peak is at 4.3 eV. On the other hand, $\Lambda(0, 0, x)$ and Σ transitions are responsible for the first peak in the theory for perpendicular polarization at 4.77 eV; the corresponding experimental peak is at 4.46 eV. The bands involved in this transition are 12, 13–18 and the critical point is near $\Gamma_5(X_5)$–$\Gamma_3(X_1)$. The main peak in the perpendicular polarization is caused by Σ transitions near the point X, bands 16-10, indicating the strong mixing of Σ and L at X in the valence bands. Our calculated peak is at 4.96 eV while experiment shows it at 4.79 eV. The small shoulder at 4.6 eV (4.17 eV in the experiment) in the perpendicular polarization is caused by a singular point at (0, 0, 0.6) along the Λ direction (bands 13–17). In this energy region we also find a critical point at (0.25, 0.25, 0) (14→17 transitions) coming from the original Σ transitions of the zb analog, these transitions are allowed only in the perpendicular polarization.

The main peak in the parallel polarization is caused by a strong critical point near (0.16, 0.5, 0), from bands (14-17). In this energy region we find two additional pieces of structure caused by a critical point at (0.25, 0.25, 0.5) in the N plane from bands 13–18 and 14–20. One structure at 5 eV appears in the parallel polarization while the other at 5.11 eV appears in the perpendicular direction. The shoulder at 4.92 eV in the experimental spectrum is associated with $\Delta(0.5, 0, 0)$ transitions from bands 15–18; our calculated value for these transitions is 5.21 eV.

IV. DISCUSSION

Table I shows the results of the critical-point analysis and a comparison with the experiment. In the dc reflectivity spectrum, the strength of the E_2 peak of $ZnGeP_2$ is considerably reduced when compared with the strength of the same peak in zincblende semiconductors. It is still higher than the measured peak, which appears to have the same strength as the E_1 peak. This, together with the fact that the width of the E_2 peak is about 0.8 eV, while our calculation shows a width of about 0.4 eV, indicates that we probably underestimated the antisymmetric cation potential for this calculation. In most other respects the structure in the experiment is very similar to our theoretical predictions. We note that by shifting the theoretical spectra by about 0.3 eV to lower energies the agreement between theory and experiment for almost all the optical structure is very good. This suggests that small changes in the form factors could give theoretical spectra in excellent agreement with experiment. This is encouraging since no experimental data (except for structure constants) were used in carrying out the calculations.

ACKNOWLEDGMENTS

We would like to thank Dr. Roger DeWames of Rockwell International Corp. for the large crystal of $ZnGeP_2$. Part of this research was done under the auspices of the Atomic Energy Commission.

---

*Supported in part by the National Science Foundation Grant No. GH 35688.

†Present address: Plinio 354, Mexico 5, D. F., Mexico.

[1]G. D. Boyd, E. Buehler, F. G. Storz, and J. H. Wernick, J. Quantum Electron. QE-8, 419 (1972).

[2]M. L. Cohen and T. K. Bergstresser, Phys. Rev. 141, 789 (1966).

[3]J. C. Phillips and J. A. Van Vechten, Phys. Rev. B 2, 2147 (1970).

[4]J. P. Walter and M. L. Cohen, Phys. Rev. 183, 763 (1969).

[5]G. Weisz, Phys. Rev. 149, 504 (1966).

[6]S. Bloom and T. K. Bergstresser, Solid State Commun. 6, 4651 (1968).

[7]R. R. L. Zucca and Y. R. Shen, Appl. Opt. 12, 1293 (1973); Y. R. Shen, Surf. Sci. 37, 522 (1973).

[8]C. Varea de Alvarez, J. P. Walter, M. L. Cohen, J. Stokes, and Y. R. Shen, Phys. Rev. B 6, 1412 (1972).

[9]S. E. Stokowski, Phys. Rev. B 6, 1294 (1972).

[10]R. DeWames (private communication).

[11]The x and y components of the $\vec{G}$ and $\vec{k}$ vectors are in units of $2\pi/a$ and the z components in units of $2\pi/c$ throughout this work.

[12]Often in this work we denote a state by its symmetry in the chalcopyrite structure (group D_{2d}^{12}, see Ref. 13) and in parentheses the symmetry of the zb state where it originates from in a perturbation approach.

[13]S. Zak, *The Irreducible Representations of Space*

Groups (Benjamin, New York, 1969).
[14]J. L. Shay, B. Tell, E. Buehler, and J. H. Wernick, Phys. Rev. Lett. 30, 983 (1973).
[15]J. E. Rowe and J. L. Shay, Phys. Rev. B 3, 451 (1971).
[16]R. A. Bendorius, G. Z. Krivaite, A. Yu. Shileika, G. F. Karavaev, and V. A. Chaldyshev, International Conference on Semiconductors, Warsaw (1992) (unpublished); A. Raudonis, V. S. Grigoreva, V. D. Prochukhan and A. Shileika, Phys. Status Solidi B 57, 415 (1973); A. Shileika, Surf. Sci. 37, 730 (1973).
[17]P. Löwdin, J. Chem. Phys. 19, 1396 (1961).
[18]G. Gilat and L. J. Raubenheimer, Phys. Rev. 144, 390 (1966).
[19]F. Herman and S. Skillman, *Atomic Structure Calculations* (Prentice Hall, Englewood Cliffs, N. J., 1966).
[20]J. J. Hopfield, J. Phys. Chem. Solids 15, 97 (1960).
[21]W. Paul, in *Proceedings of the Colloquium on the Physical Properties of Solids under Pressure, Grenoble*, 1969 (Centre National de la Recherche Scientifique, Grenoble, 1970), p. 199.
[22]J. L. Shay, E. Buehler, and J. H. Wernick, Phys. Rev. B 2, 4104 (1970); 3, 2004 (1971); J. L. Shay and E. Buehler, *ibid.* 3, 2598 (1971); 4, 2479 (1971); C. C. Y. Kwan and J. C. Woolley, Can. J. Phys. 48, 2085 (1970); Phys. Status Solidi B 44, K93 (1971); Appl. Phys. Lett. 18, 520 (1971); R. K. Karymshakov, Y. I. Ukhanov, and Y. V. Shmartsev, Fiz. Tekh. Poluprov. 5, 514 (1971) [Sov. Phys.-Semicond. 5, 450 (1971)].
[23]J. Kavaliauskas, G. F. Karavaev, E. I. Leonov, V. M. Orlov, V. A. Chaldyshev, and A. Shileika, Phys. Status Solidi B 45, 443 (1971).